DIRECT OBSERVATION OF THE LIFT-UP EFFECT IN BOUNDARY LAYER TRANSITION USING HYDROGEN-BUBBLE METHOD

Ayumu Inasawa
Dept. of Aerospace Eng., Tohoku Univ.,
Aramaki-Aoba 01, Aoba-ku, Sendai 980-8579, Japan
ainasawa@ltwt.ifs.tohoku.ac.jp

Fredrik Lundell
Dept. of Mech., KTH,
S-100 44 Stockholm, Sweden
fredrik@mech.kth.se

Masaharu Matsubara
Dept. of Mech. Eng., Shinshu Univ.
Wakasato 4-17-1, Nagano 380-8553, Japan
mmatsu@gipwc.shinshu-u.ac.jp

Yasuaki Kohama
Institute of Fluid Science, Tohoku Univ.,
Katahira 2-1-1, Aoba-ku, Sendai 980-8577, Japan
kohama@ifs.tohoku.ac.jp

ABSTRACT

Transition of a boundary layer subjected to free-stream turbulence has been studied in a water-channel. A stereo PIV-system (Particle Image Velocimetry) using hydrogen bubbles as particles has been developed and validated against 1D LDV (Laser Doppler Velocimetry) measurements. It is well known that the disturbances of the free-stream turbulence generate streamwise elongated regions of low streamwise velocity in the boundary layer. The elongated regions, or streaks, develop downstream and eventually breaks down to turbulence after the appearance of wavy secondary instabilities, seen in flow visualizations. In the present study, the lift-up mechanism, creating large amplitude streamwise velocity disturbances, is studied. Lift-up is the transport of low velocity fluid from close to the wall to higher regions of the boundary layer by a small wall-normal velocity disturbance, induced by the free-stream turbulence. Stereo PIV using two synchronized video cameras gives instantaneous spanwise distributions of the streamwise and the wall-normal velocities, showing a strong negative correlation between the wall-normal and streamwise velocities in the centre of the boundary layer. This demonstrates the lift-up effect from direct velocity measurements.

INTRODUCTION

If a laminar boundary layer is exposed to enhanced levels of free-stream turbulence (FST), the transition scenario is different from single mode Tollmien-Shlichting (T-S) waves dominated scenarios. In the FST case, the disturbances of the free-stream turbulence generate streamwise low-speed streaks in the boundary layer and these structures develop downstream and eventually breakdown to turbulence occurs after wavelike secondary instabilities of the streaks. Work on FST induced transition has been reviewed by Kendall (1998) and recently Matsubara & Alfredsson (2001) reported detailed hot-wire measurements of disturbances in a boundary-layer subjected to various levels of FST.

Theoretically, it has been shown (Andersson

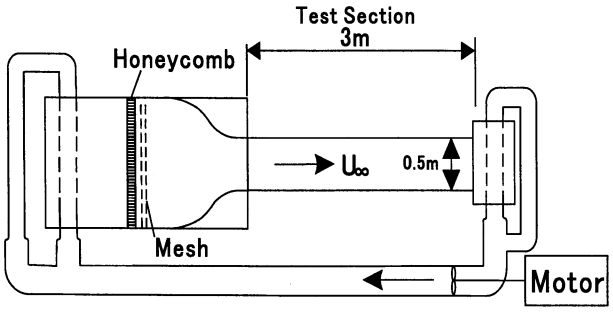

Figure 1: Water tunnel.

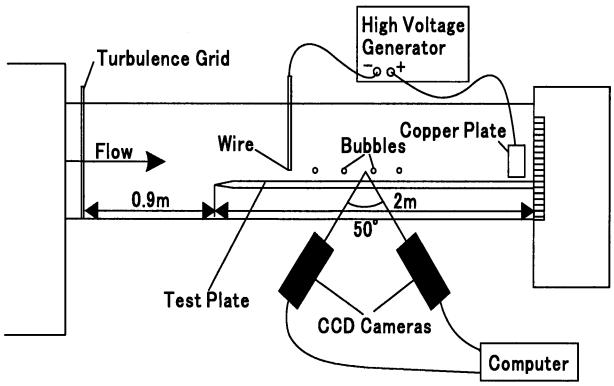

Figure 2: Experimental set-up.

et al. (1999) & Luchini (2000)) that, due to the non-orthogonality of the eigenmodes to the coupled Orr-Sommerfeld and Squire equations, disturbances can exhibit an initial amplification considerable stronger than the growth of single TS-wave modes. Provided that the initial disturbance is strong enough, transition might be governed by the transient growth of multi-mode disturbances. Such disturbances typically have the form of weak streamwise vortices which downstream generate strong streamwise streaks. The wall-normal disturbance distributions obtained from theory is in good agreement with experimental results.

The strong streamwise-velocity disturbance is created by the streamwise vortices, which, with their wall-normal velocity component, move low speed fluid from close to the wall to further out in the boundary layer, thus creating a low-speed disturbance. The wall-normal velocity is small as compared to the streamwise velocity and this fact, together with the moving spanwise velocity gradients, makes direct measurements of the wall-normal velocity very difficult to perform with hot-wire probes.

The purpose of the present study is to perform direct measurements of the lift-up mechanism using hydrogen-bubble visualizations in water. Two synchronized cameras take simultaneous images of bubble lines created by a tungsten wire from different viewing angles. Using stereo PIV methods, the u and v velocities can be obtained form those images.

EXPERIMENTAL SET-UP

The experiments were carried out in a water tunnel (figure 1). The contraction ratio is 4:1 and the test section width, height and length are 500, 500 and 3000 mm, respectively. The side and bottom walls of the test section are made of glass in order to simplify visualizations. A schematic of the experimental set-up is seen in figure 2. In the channel, a flat plate, made of acrylic and 2095 mm long was inserted. The plate had a 95 mm long, separately manufactured leading edge made of aluminium. The leading edge was wedge-shaped with vertical angle, streamwise length and thickness 3°, 95 mm and 10 mm, respectively. The coordinate system is x for the streamwise direction, where $x = 0$ is at the plate leading edge, y for the coordinate normal to the plate with $y = 0$ at the plate, and z as the spanwise coordinate.

The plate was put 110 mm above the bottom wall of the test section. The free-stream turbulence was generated by an active turbulence grid made of 5 mm aluminium pipes. The distance from the grid to the leading edge was 900 mm. In order to control the free-stream turbulence level, 1 mm holes were drilled in the aluminium bars towards the upstream direction. The turbulence intensity can be changed by the amount of water pressed through the holes. The grid mesh width and hole interval are both 40 mm. The free-steam turbulence level could also be increased by moving the turbulence grid closer to the leading edge.

MEASUREMENT TECHNIQUE

Flow visualizations were done with hydrogen bubbles. A 0.05 mm tungsten wire was used as cathode and a copper plate placed downstream of the measurement position as anode. A voltage of 400 V was needed to create clear bubble lines. By pulsing the wire voltage, hydrogen bubble lines were produced. The bubble lines were filmed by two progressive scan cameras positioned under the test section. The two cameras captured images of the bubble lines from the same area under different angles. The cameras were synchronized with the hydrogen bubble lines and the images were captured to a computer by an AD capture-board.

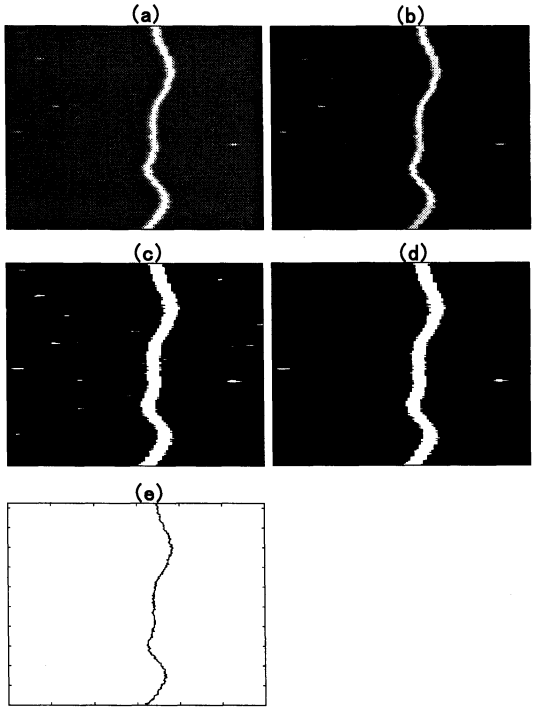

Figure 3: Sequence of image analysis.

Figure 3 shows how the accurate position of a bubble line was obtained from a captured image. The original raw image is shown in figure 3 (a). Flow is from left to right and a wavy bubble-line is seen in the middle of the image. The evaluation process is shown in the sequence (b) to (e). First, the contrast of each row of the image was enhanced (figure 3 (b)). Thereafter, a threshold was used in order to obtain a binary image as seen in figure 3 (c). As seen in the figure, not only the bubble line passes the threshold, but also some noise from dust in the water. In order to remove the noise, a labeling method, which removes white pixels which are not neighbours to other white pixels, was used. The result after this step is shown in (d). Finally, the position of the bubble line was taken to be the centre of the thick white line in figure 3 (d). The final result is seen in figure 3 (e).

Typical images from the two cameras obtained during measurements are shown in figure 4. The size of the area shown is 95 mm in the streamwise (horizontal) and 74 mm in the spanwise (vertical) directions, respectively. The bubble wire was positioned in the centre of the boundary layer and flow is from left to right. Two low-speed streaks are seen, one slightly above the middle and one 1/4 way up from the bottom of the images. Since the two images are taken from different viewing angles (from the upstream direction in (a) and downstream in (b)), stereo PIV-techniques gives the possibility to obtain not only the streamwise position (x) of the bubble-lines but also the vertical position (y).

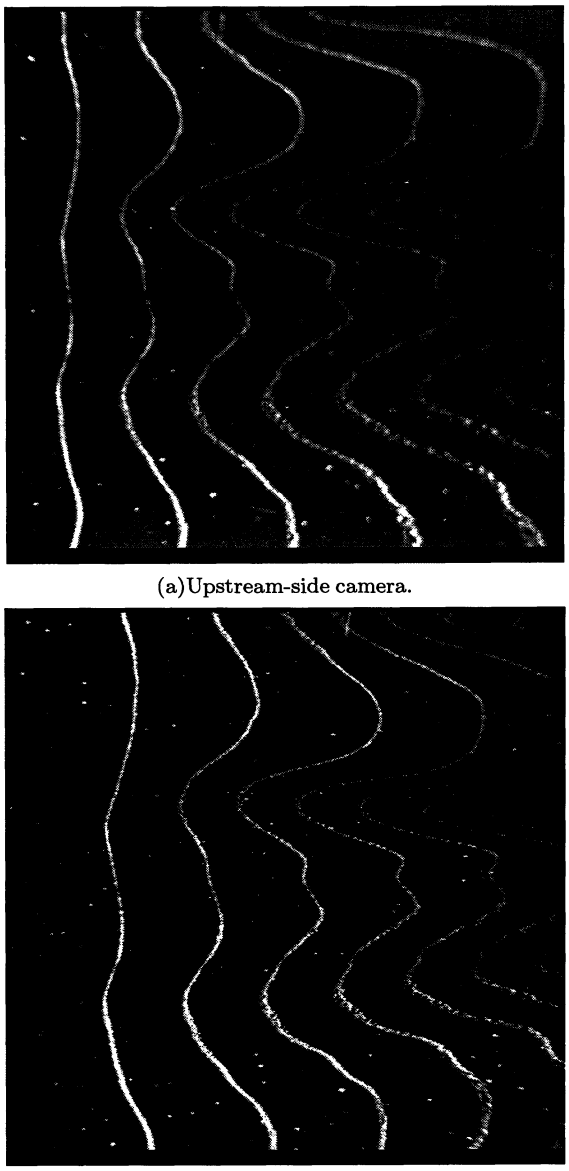

(a)Upstream-side camera.

(b)Downstream-side camera.

Figure 4: Original images.

From the thus obtained x and y positions of the bubble lines and the known time interval between them, the streamwise velocity $u(z)$ and wall-normal velocity $v(z)$ were calculated, averaging over the image in the streamwise (horizontal) direction. Free-stream velocity and turbulence intensity were measured by a LDV (Laser Doppler Velocimetry) system, whose measurement volume was positioned 100 mm above the tip of leading edge.

RESULTS AND DISCUSSION

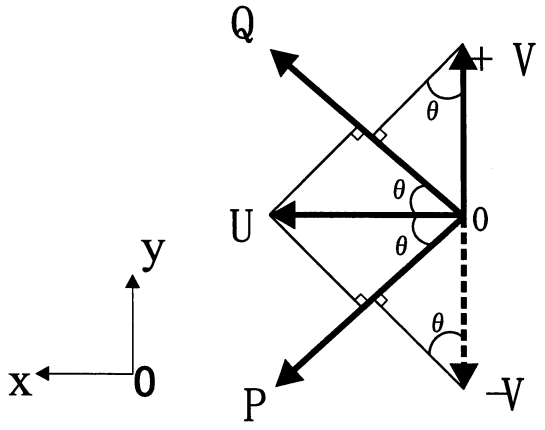

Figure 5: Principle of v_{rms} evaluation using one-component LDV system.

Method	U_{mean} (m/s)	u_{rms} (m/s)	v_{rms} (m/s)	$u'v'$ (m^2/s^2)
LDV	0.07367	0.00616	0.00315	-5.14×10^{-5}
Image	0.07490	0.00594	0.00324	-5.41×10^{-5}
Discrepancy	1.7%	3.35%	4.2%	5.3%

Table 1: Comparison between LDV and stereo PIV measurements.

Validity of imaging data

In order to confirm the accuracy of the stereo-PIV system described above, one-dimensional LDV measurements were made. Figure 5 illustrates the principle of v_{rms} and $u'v'$ evaluation by the one-component LDV system used. The velocities P and Q are given by U and V as:

$$P = Ucos\theta + Vsin\theta \quad (1)$$

$$Q = Ucos\theta - Vsin\theta \quad (2)$$

Each velocity component is divided into a mean and a fluctuating component, i.e. U is denoted as

$$U = \overline{U} + u' \quad (3)$$

where $\overline{U}$ is a constant and u' has zero mean. Inserting the decomposed velocity components into the equations (1) and (2), raising to the second power, taking time-average of each equation and subtracting the equations for the mean value the following equations are obtained. The variables now denote their time average so that $u'^2 = u_{rms}^2$.

$$p'^2 = u'^2cos^2\theta + 2u'v'sin\theta cos\theta + v'^2sin^2\theta \quad (4)$$

$$q'^2 = u'^2cos^2\theta - 2u'v'sin\theta cos\theta + v'^2sin^2\theta \quad (5)$$

Measuring the velocities U, P and Q separately, the wall-normal velocity fluctuation is obtained by adding equations (4) and (5).

$$v'^2 = \frac{1}{2sin^2\theta}(p'^2 + q'^2 - 2u'^2cos^2\theta) \quad (6)$$

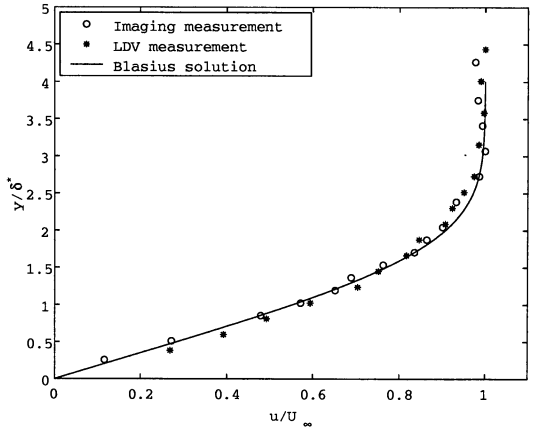

(a)Mean velocity profile.

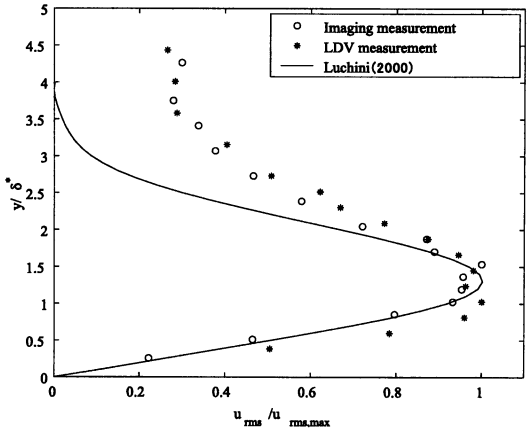

(b)u_{rms} distribution.

Figure 6: Stereo PIV measurements inside the Boundary layer. $x = 800$ mm, $U_\infty = 0.09$ m/s and $Tu = 3.3\%$.

Similarly, subtraction of equation (4) and (5) gives the $u'v'$ correlation.

In order to check the accuracy of the stereo PIV-data, measurements were performed in the free stream. At each angle, the LDV signal was sampled with a frequency and sampling time of 200 Hz and 600 s, respectively. For the stereo PIV, 1000 double images taken with a frequency of 6 Hz were used for evaluating data. The calibration data are shown in table 1. As can be seen, the discrepancy between stereo PIV and LDV is 5 % or lower, showing a decent accuracy of the stereo PIV method.

Boundary layer measurements

The boundary layer characteristics at $x = 800$ mm and a free stream velocity (U_∞) of 0.09 m/s are shown in figure 6. The turbulence level at the leading edge was 3.3/The height was varied by traversing the bubble wire through the boundary layer. The velocity profile is seen to agree well with the Blasius profile

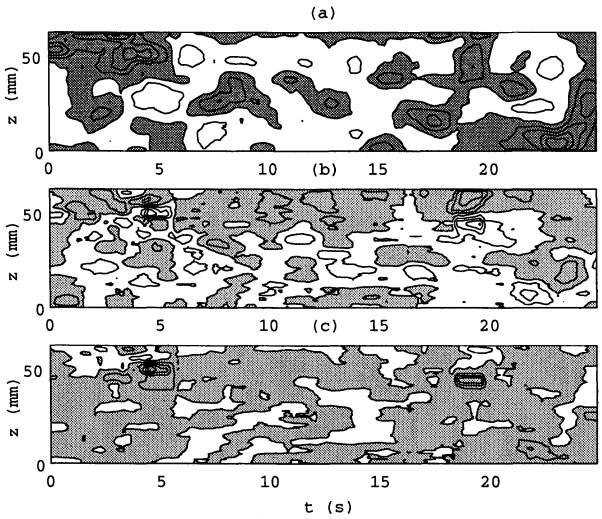

Figure 7: Contour maps of u, v and $u \cdot v$ at $y/\delta^* = 3$. Negative value region is filled in gray. (a) u, (b) v, (c) $u \cdot v$ correlation. Contour spacings are 5 mm/s, 1.5 mm/s and 25 mm^2/s^2, respectively

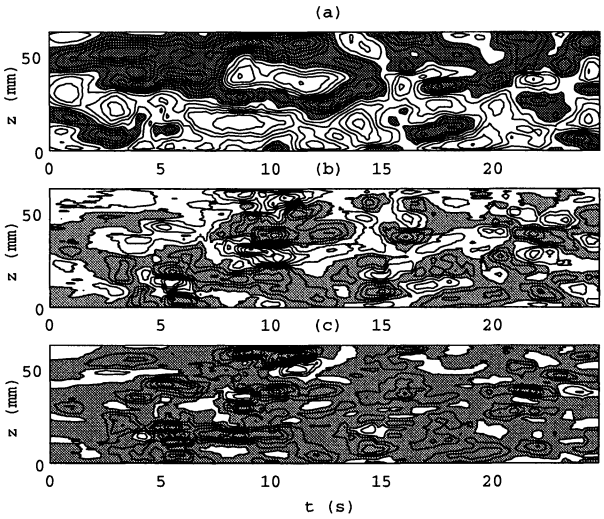

Figure 8: Contour maps of u, v and $u \cdot v$ at $y/\delta^* = 1.3$. Negative value region is filled in gray. (a) u, (b) v, (c) $u \cdot v$ correlation. Contour spacings are 5 mm/s, 1.5 mm/s and 25 mm^2/s^2, respectively

and the disturbance profile fits the theoretical distribution calculated by Luchini (2000) well. The agreement between measurements and theory in this case is well established, as seen in Andersson *et al.* (1999), Matsubara & Alfredsson (2001) and Luchini (2000).

Direct observation

During the reported measurements, the free-stream velocity and turbulence level at the leading edge was 0.12 m/s and 3.3% respectively. The Reynolds number based on distance from tip of leading edge to the stereo PIV measurement area at $x = 900$ mm was 1.1×10^5.

When watching the bubbles, lift up of the bubble lines in the low-speed regions could be observed by the eye, a beautiful and striking effect difficult to capture on single, flat photographs. Therefore, the stereo PIV system was developed so that the effect could be quantified.

Figures 7–9 show contour maps of u, v, and uv at various heights in the boundary layer. Negative values are filled in gray. At each height, 100 double image sets were used and for each time, the velocity is averaged over the streamwise extent of the measured area. It should be emphasized that the measurements at different *heights* were not simultaneous, why no comparisons of individual structures can be made in figures 7–9.

In (a) of figures 7–9, the streamwise velocity disturbance is shown. At $y/\delta^* = 1.3$, figure 8 (a), strong low speed (gray) velocity streaks are

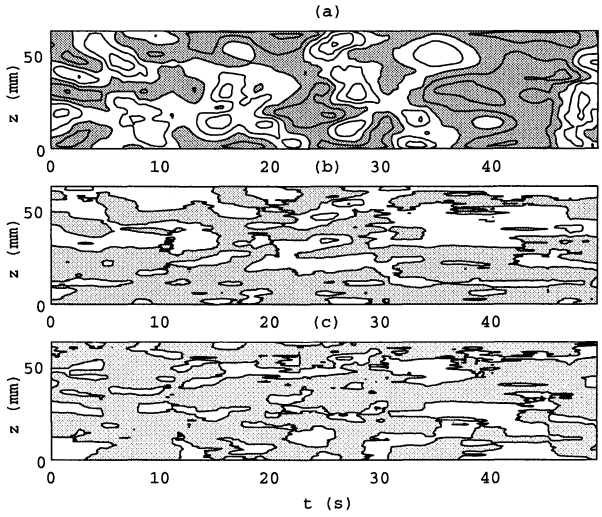

Figure 9: Contour maps of u, v and $u \cdot v$ at $y/\delta^* = 0.3$. Negative value region is filled in gray. (a) u, (b) v, (c) $u \cdot v$ correlation. Contour spacings are 5 mm/s, 1.5 mm/s and 25 mm^2/s^2, respectively

clearly seen. At the other heights, low speed structures are much less accentuated.

As seen in figures 7–9 (b), the vertical, v, velocity is seen to be particularly high (white) at $y/\delta^* = 1.3$ as well. Comparing figures 8 (a) and (b), it can be suspected that a positive v velocity corresponds to a negative disturbance in u. This suspicion is confirmed when studying the uv distribution in figure 8 (c), where very strong negative (gray) correlations are seen at the positions of the low speed streaks in (a). At the other heights, figures 9 and 7 (c), uv are not at all correlated as strong as at the centre of the boundary layer.

The strong negative correlation in uv thus confirm that lift up is the mechanism behind the strong, negative, elongated streamwise velocity disturbance seen in FST induced transition.

Acknowledgments

Mr. Yamabe is a patient teacher and an excellent craftsman in the workshop. Fredrik Lundell's stay in Japan was partly financed by the Scandinavia-Japan Sasakawa Foundation.

REFERENCES

Andersson, P., Berggren, M. & Henningson, D. S. 1999, "Optimal disturbances and bypass transition in boundary layers", *Phys. Fluids.* **11** pp. 134–150

Butler, K. M. & Farrell, D. F. 1992, "Three dimensional optimal perturbations in viscous shear flow", *Phys. Fluids A* **4**, pp. 1637–1650

Ellingsen, T & Palm, E. 1975, "Stability of linear flow", *Phys. Fluids.* **18**, p. 487

Kendall, J. M. 1998, "Experiments on boundary layer receptivity to freestream turbulence", AIAA-paper 98-0530

Landahl, M. T. 1980, "A note on an algebraic instability of inviscid shear flows", *J. Fluid Mech.* **98**, pp. 243–251

Luchini, P. 2000, "Reynolds number independent instability of the boundary layer over a flat surface: optimal perturbations", *J. Fluid Mech.* **404** pp. 289–309

Matsubara, M. & Alfredsson, P. H. 2001, "Disturbance growth boundary layers subjected to free-stream turbulence", *J. Fluid Mech.* **430** pp.149–168